

Supporting Information

Carbon Dot-Sensitized MoS₂ Nanosheet Heterojunctions as Highly Efficient NIR Photothermal Agents for Complete Tumor Ablation at Ultralow Laser Exposure

Bijiang Geng,^{‡a} Hua Qin,^{‡a} Fengfeng Zheng,^{‡a} Wenwen Shen,^a Ping Li,^d Kuan Wu,^a Xulong Wang,^a Xiaokai Li,^{*b} Dengyu Pan,^{*a} and Longxiang Shen^{*c}

^aSchool of Environmental and Chemical Engineering, Shanghai University, Shanghai 200444, P.R. China

^bPhysical Education College, Shanghai University, Shanghai 200444, P.R. China

^cDepartment of Orthopedic Surgery, Shanghai Jiao Tong University affiliated Sixth People's Hospital, Shanghai 200233, P.R. China

^dSchool of Life Sciences, Shanghai University, Shanghai 200444, P.R. China

[‡]These authors contributed equally to this work.

Supporting Experimental Section

Preparation of NIR-CDs

1,3,6-trinitropyrene (TNP) was first prepared through the nitration reaction of pyrene (purity>98%) following our previous report.¹ Then, the NIR-responsive CDs (NIR-CDs) were synthesized via a hydrothermal process using TNP and BPEI₁₈₀₀ as the precursors. Specifically, 0.1 g TNP and BPEI were dispersed in 40 mL DI water by ultrasonication, and then this solution was transferred into a 100 mL poly(tetrafluoroethylene)-lined autoclave. The amount of BPEI was varied from 0.4 to 1.6 g and the molecular weight of BPEI was varied from 600 to 10000, while the amount of TNP remained constant (0.1 g). A crude product containing NIR-CD aqueous solution was derived after heated at 200 °C in an oven for 12 h. The obtained NIR-CDs were purified by filtration and dialysis to remove unreacted precursors. Finally, a black NIR-CD aqueous solution was obtained.

Preparation of PEG-functionalized single-layer MoS₂ nanosheets

MoS₂ nanosheets were synthesized by a facile hydrothermal route as previously reported.² Briefly, 300 mg (NH₄)₂MoS₄ was dissolved into a mixture solution, which contains 30 mL PEG-400 and 30 mL distilled water, and then the mixture solution was transferred into a 100 mL poly(tetrafluoroethylene)-lined autoclave. The MoS₂ nanosheets were obtained after the hydrothermal reaction for 12 h at 220 °C in an oven and purified by washing with monoethanolamine solution (50%, in water, v/v) and distilled water for several times.

Preparation of NIR-CD/MoS₂ heterojunctions

The NIR-CD/MoS₂ heterojunctions were synthesized by depositing the NIR-CDs (0.4 mg mL⁻¹) onto the surface of the MoS₂ nanosheets (0.2 mg mL⁻¹) under vigorous stirring at room temperature in PBS (20 mM, pH=8.0). After stirring for 24 h, excess unbounded NIR-CDs were washed away by centrifugation and repeatedly for several times, obtaining NIR-CD/MoS₂ heterojunctions dispersed in water for future use.

The loading ratio of NIR-CDs were determined by the changed mass of MoS₂ nanosheets before and after NIR-CD loading. The loading ratio of NIR-CDs was calculated based on the following equation:

$$\text{Loading ratio (\%)} = \frac{m_2 - m_1}{m_1}$$

where m_1 was the mass of MoS₂ and m_2 represented the total mass of NIR-CD/MoS₂.

Characterization

Transmission electron microscopy (TEM) images were recorded on a JEM-2100F microscope operated at 200 kV acceleration voltage using the super thin carbon films. X ray diffraction (XRD) patterns were obtained

with a Rigaku 18 KW D/max-2550 using Cu K α radiation. Fourier transform infrared (FT-IR) spectra of dried samples were collected using a Nicolet AVATAR 370 FT-IR. X-ray photoelectron spectroscopy (XPS) measurements were performed using a Kratos Axis Ultra DLD X-ray photoelectron spectrometer. Zeta potential and dynamic light scattering (DLS) were acquired from a Malvern Zetasizer Nano ZS90 Zeta potential analyzer. UV-vis-NIR absorption spectra were obtained by a Hitachi 3100 spectrophotometer, and fluorescence spectra were carried out using a Hitachi 7000 fluorescence spectrophotometer. Time-resolved fluorescence spectra were gained using a FLS920 time-corrected single photon counting system.

Electrochemical measurements

The cyclic voltammetry (CV) was performed by using a conventional three-electrode system on a CHI 660D electrochemical workstation (Chenhua Instrument, Shanghai, China), which consists of a NIR-CD coated platinum sheet as the working electrode, a platinum wire as the counter electrode, and an Ag/AgCl (saturated KCl) as the reference electrode. CV was recorded in acetonitrile containing 0.1 M TBAPF₆ as the supporting electrolyte. The lowest unoccupied molecular orbital (LUMO) energy level of the NIR-CDs was calculated according to the following equation: $E_{\text{LUMO}} = -e(E_{\text{red}} + 4.4)$ (eV).

Photothermal Performance of NIR-CD/MoS₂ heterojunctions

Photothermal performance of NIR-CD/MoS₂ heterojunctions was obtained by irradiating a centrifuge tube containing a dispersion of NIR-CD/MoS₂ (0, 0.0375, 0.075, 0.15, 0.3, and 0.6 mg mL⁻¹). 1 mL of NIR-CD/MoS₂ solution was irradiated with the laser (808 nm) for 5 min, the power density is 0.2 W cm⁻². The temperature of NIR-CD/MoS₂ solution was measured and recorded every 30 s by the Fluke infrared thermal imaging camera. The photostability of NIR-CD/MoS₂ heterojunctions were investigated by monitoring their absorbance changes under the laser irradiation (808nm, 0.2 W cm⁻²). The photothermal performance of pristine MoS₂ (0.6 mg mL⁻¹) and NIR-CDs (0.6 mg mL⁻¹) were also investigated at the same laser power density (0.2 W cm⁻²).

Calculation of the photothermal conversion efficiency of NIR-CD/MoS₂ heterojunctions

The temperature changes of the NIR-CD/MoS₂ (0.6 mg mL⁻¹) as a function of time under the laser irradiation (808 nm, 0.2 W cm⁻²) were recorded to evaluate the photothermal conversion efficiency. Following the report of Roper et al.,³ photothermal conversion efficiency (η) was calculated using equation (1).

$$\eta = \frac{hA(T_{\text{max}} - T_{\text{surr}}) - Q_{\text{Dis}}}{I(1 - 10^{-A\lambda})} \quad (1)$$

Where h and A represents the heat transfer coefficient and the surface area of the container, respectively. T_{surr}

(29.3 °C) and T_{max} (55.0 °C) indicates the ambient temperature and the equilibrium temperature, respectively. The 808 nm absorbance of NIR-CD/MoS₂ (A_λ) is 2.001. The incident 808 nm laser power density (I) is 0.2 W cm⁻². Therefore, the hA in the equation (1) is unknown. In order to obtain hA , a dimensionless parameter (θ) and a time constant of sample system (τ_s) are introduced and acquired by following equation (2) and (3).

$$\theta = \frac{T - T_{surr}}{T_{max} - T_{surr}} \quad (2)$$

$$\tau_s = \frac{m_D c_D}{hA} \quad (3)$$

Where c_D and m_D are the heat capacity (4.2 J g⁻¹) and the mass (0.6 g). Following equation (4), we can determine the time constant (τ) by applying the linear time data from the cooling period versus $\ln\theta$

$$t = -\tau(\ln \theta) \quad (4)$$

Therefore, the time constant (τ_s) was determined to be 341.0 s. According to the equation (3), hA can be determined. Therefore, the photothermal conversion efficiency (η) at 808 nm of NIR-CD/MoS₂ can be calculated to be 78.2%. For pristine NIR-CDs (0.6 mg mL⁻¹) and MoS₂ (0.6 mg mL⁻¹), the η can be calculated to be 37.6% and 38.3%, respectively.

DOX Loading and releasing

NIR-CD/MoS₂ heterojunctions were mixed with DOX (0.1 mg mL⁻¹, 2 mL) in PBS (20 mM, pH=8.0). After stirring for 24 h at room temperature, excess unbounded DOX were removed by centrifugation and repeatedly for several times. The obtained NIR-CD/DOX/MoS₂ were re-dispersed in aqueous solution and stored at 4 °C for further use.

Before and after the DOX loading, the UV-vis-NIR spectra of NIR-CD/MoS₂ were recorded to determine the loading ratio of DOX. After the absorbance contributed from NIR-CD/MoS₂ was subtracted from the spectra of NIR-CD/DOX/MoS₂, the absorbance at 488 nm was used to measure the concentration of DOX. The drug loading (DL) of DOX was calculated based on the following equation:

$$DL(\%) = \frac{m_e}{m_t}$$

where m_e was the mass of loaded DOX (0.2 mg) and m_t represented the total mass of NIR-CD/DOX/MoS₂ (0.8 mg). Therefore, the DL of DOX on the heterojunction was calculated to 25%.

The drug release kinetics at pH=5.0, 6.5, and 7.4 were carried out through dialysis method. Briefly, NIR-CD/DOX/MoS₂ (1 mL) was encapsulated in a dialysis bag (MWCO = 14 kDa) and then immersed within 19

mL PBS. Then, 2 mL of the outside solution was collected at different time points and measured by the spectrophotometer to measure the concentration of released DOX. After measured, the solution was poured back to dialysis bag to ensure the constant volume.

Cell culture

Hela and 4T1 cells were cultured in Dulbecco's modified Eagle's medium (DMEM) and Roswell Park Memorial Institute-1640 (RPMI 1640) supplemented with 10% heat-inactivated fetal bovine serum (FBS, Gibco) at 37 °C in 5% CO₂/95% air atmosphere, respectively. All cell lines used in this paper were ordered from the Chinese Academy of Sciences and cultured following the protocol.

LDH release assay

Cell membrane integrity of cells exposed to NIR-CD/MoS₂ was tested using lactate dehydrogenase (LDH) test-kit (Beyotime Institute of Biotechnology, China). Hela cells were plated in 96-well plates (5×10³ cells per well) and allowed to adhere overnight. NIR-CD/MoS₂ were introduced separately to the cells with different concentrations (37.5, 75, 150, 300 and 600 μg mL⁻¹) and incubated for 24 h. The positive control was prepared by adding 10 μL lysis solution to the cells at 1 h prior to the centrifugation. After centrifugation (400 rpm×5 min), 120 μL supernatant was taken out from each well for LDH assay, following the instruction of the kit. The absorbance at 490 nm was recorded on a Microplate Reader (Thermo, USA). The LDH leakage (% of positive control) is expressed as the percentage of $(OD_{\text{test}} - OD_{\text{blank}})/(OD_{\text{positive}} - OD_{\text{blank}})$, where OD_{test} is the optical density of the control cells or cells exposed to NIR-CD/MoS₂, OD_{positive} is the optical density of the positive control cells and OD_{blank} is the optical density of the wells without Hela cells.

ROS Level assay

Reactive oxygen species (ROS) level was detected using 2',7'-dichlorofluorescein diacetate (DCFH-DA, Beyotime, China), which can enter cells and be hydrolyzed into a fluorescent 2',7'-dichlorofluorescein (DCFH) probe. After seeded into 96-well plates with a density of 5000 cells per well and grown overnight, Hela cells was cultured in the fresh medium containing NIR-CD/MoS₂ with different concentrations for 24 h. The positive controls were prepared with Hela cells cultured in fresh medium containing H₂O₂ for 20 min prior to the addition of DCFH-DA. Then the ROS levels were determined following the protocol, using a Microplate Reader (Thermo, USA). The ROS level is expressed as the ratio of $(OD_{\text{test}} - OD_{\text{blank}})/(OD_{\text{positive}} - OD_{\text{blank}})$, where OD_{test} is the fluorescence intensity of the cells exposed to NIR-CD/MoS₂, OD_{positive} is the fluorescence intensity of the cells exposed to positive control (H₂O₂) and OD_{blank} is the fluorescence intensity of the wells without Hela cells.

We further utilized the fluorescence microscope to detect the ROS level. HeLa cells seeded into a 6-well plate were firstly incubated in the fresh medium containing NIR-CD/MoS₂ with different concentrations for 24 h. Then, the excessive NIR-CD/MoS₂ was washed out with PBS and then the cells were incubated with a culture medium containing DCFH for another 20 min in the dark. The positive control cells were treated with 200 μL of H₂O₂ at 37 °C for 20 min. Fluorescence images were immediately measured on an Olympus BX53 fluorescence microscope (Olympus, Japan) with an excitation wavelength of 488 nm and an emission wavelength of 515-540 nm.

Observation of pH-triggered DOX release by *in vitro* fluorescence imaging

HeLa cells (2×10^5) were seeded in culture dishes and incubated for at least 24 h at 37 °C under 5% CO₂/95% air. The DOX loaded NIR-CD/MoS₂ solution was added into the cells and examined under a confocal laser scanning microscope (Olympus, Japan) using lasers of 561 nm. The fluorescence signal was collected at 600–700 nm, respectively. For pH-triggered release of DOX, the HeLa cells were incubated with NIR-CD/DOX/MoS₂ at pH=6.5 for 5 min, and then the cells were examined under a confocal laser scanning microscope.

***In vitro* cytotoxicity assays**

The cell viabilities of NIR-CD, MoS₂, and NIR-CD/MoS₂ were determined by MTT assay. The HeLa cells were cultured in a 96-well plate (4×10^3 cells per well). After adhering overnight, the DMEM was taken out and a fresh DMEM medium containing various concentration of NIR-CD/MoS₂ (0.0375, 0.075, 0.15, 0.3 and 0.6 mg mL⁻¹) were added for an incubation for 24 h and 48 h. After that, 20 μL of MTT was added into the wells. The medium was removed after another 4 h incubation and 150 μL of DMSO was added into the cells. Absorbance at 490 nm of each well was measured via a Microplate Reader (Thermo, USA). The free NIR-CDs and MoS₂ were used as a control.

***In vitro* PTT and PCT**

To study the *in vitro* PTT efficiency of NIR-CD/MoS₂ and PCT efficiency of NIR-CD/DOX/MoS₂, the viabilities of HeLa cells after various treatments were measured by MTT assays. As previously described, HeLa cells were cultured in a 96-well plate (4×10^3 cells per well). After adhering overnight, the DMEM was taken out and a fresh DMEM medium containing various concentration of NIR-CD/MoS₂ (0.0375, 0.075, 0.15, 0.3 and 0.6 mg mL⁻¹) were added for another 4 h incubation. Then, the HeLa cells were irradiated by the laser (808 nm, 0.2 W cm⁻²) for 5 min. Then, the MTT assay was conducted. Absorbance at 490 nm of each well was measured via a Microplate Reader (Thermo, USA). The PCT group of NIR-CD/DOX/MoS₂ under the laser

irradiation (808 nm, 0.1 W cm⁻²) was also performed.

Xenograft tumor model

Female Balb/c nude mice with the age of 4-6 weeks were purchased from the SLAC Laboratory Animal Co. Ltd. (Shanghai, China). 0.1 mL of 4T1 cell suspension (2×10⁶ cells) was subcutaneous injection into the axillary of nude mice to generate a tumor model.

In vitro and in vivo CT imaging

The CT imaging was conducted on a SkyScan 1176 high resolution in-vivo X-ray microtomograph (Bruker). For *in vitro* CT imaging, the MoS₂ nanosheets were diluted into different concentrations and then managed in a line for CT imaging measurements at the voltage of 80 kV. For *in vivo* CT imaging, mice bearing 4T1 tumors were intravenously injected with MoS₂ (1.0 mg mL⁻¹, 200 μL). At 0 and 24 h post-injection, the mice were anaesthetized and imaged.

In vivo PTT and PCT

When the tumor volume reached approximately 100 mm³, mice were randomly divided into seven groups (five mice per group). Group 1: Saline; Group 2: NIR-CD/DOX/MoS₂; Group 3: Free DOX; Group 4: Saline + 808 nm laser (0.2 W cm⁻², 5 min); Group 5: MoS₂ + 808 nm laser (0.2 W cm⁻², 5 min); Group 6: NIR-CD/MoS₂ + 808 nm laser (0.2 W cm⁻², 5 min); Group 7: NIR-CD/DOX/MoS₂ + 808 nm laser (0.1 W cm⁻², 5 min). Fluke infrared thermal imaging camera was used to monitor the temperature changes of tumor sites during the laser irradiation. The body weight and the volume of the tumors were measured every day and every other day, respectively. The tumor volume was determined according to the following equation: $V = (A \times B^2) / 2$, where A is the maximum diameter and B is the minimum diameter of the tumor.

Histology measurements and blood analysis

The mice bearing 4T1 tumors were divided into seven groups and sacrificed at the end of the treatment (18 days). Major organs were collected and stained by H&E. Then, the images were collected by a digital microscope (Leica QWin). Blood was collected from the orbital of treated mice for serum biochemistry assay and complete blood panel analysis, which were conducted by Wuhan Saiweier Biological Technology Co., Ltd.

Hemolysis Assay

5 mL of fresh ethylenediamine tetraacetic acid (EDTA)-stabilized human whole blood obtained from volunteer was added to 10 mL of calcium- and magnesium-free Dulbecco's phosphate buffered saline (PBS). Then, RBCs were isolated from serum by centrifuging at 500 g for 10 min and repeated for five times. After

washed and diluted in 50 mL PBS, the RBC suspension (0.2 mL) was added to NIR-CD/DOX/MoS₂ solution (0.8 mL). The final concentration of NIR-CD/DOX/MoS₂ solutions ranges from 0.0375-0.6 mg mL⁻¹. The positive control and negative control group was DI water and PBS, respectively. After incubation at 37 °C for 3 h, the samples were centrifuged at 10000 g for 3 min. The hemoglobin absorbance in the supernatant was measured at 540 nm, with 655 nm as a reference. Percent hemolysis was calculated using equation (1).

$$\text{percent hemolysis (\%)} = \left(\frac{\text{sample } abs_{540 - 655 \text{ nm}} - \text{negative control } abs_{540 - 655 \text{ nm}}}{\text{positive control } abs_{540 - 655 \text{ nm}} - \text{negative control } abs_{540 - 655 \text{ nm}}} \right) \times 100 \quad (1)$$

References

1. L. Wang, Y. Wang, T. Xu, H. Liao, C. Yao, Y. Liu, Z. Li, Z. Chen, D. Pan, L. Sun, M. Wu, *Nat. Commun.*, 2014, **5**, 5357.
2. S. Wang, K. Li, Y. Chen, H. Chen, M. Ma, J. Feng, Q. Zhao, J. Shi, *Biomaterials*, 2015, **39**, 206-217.
3. D. K. Roper, W. Ahn, M. Hoepfner, *J. Phys. Chem. C.*, 2007, **111**, 3636-3641.

Supporting Figures

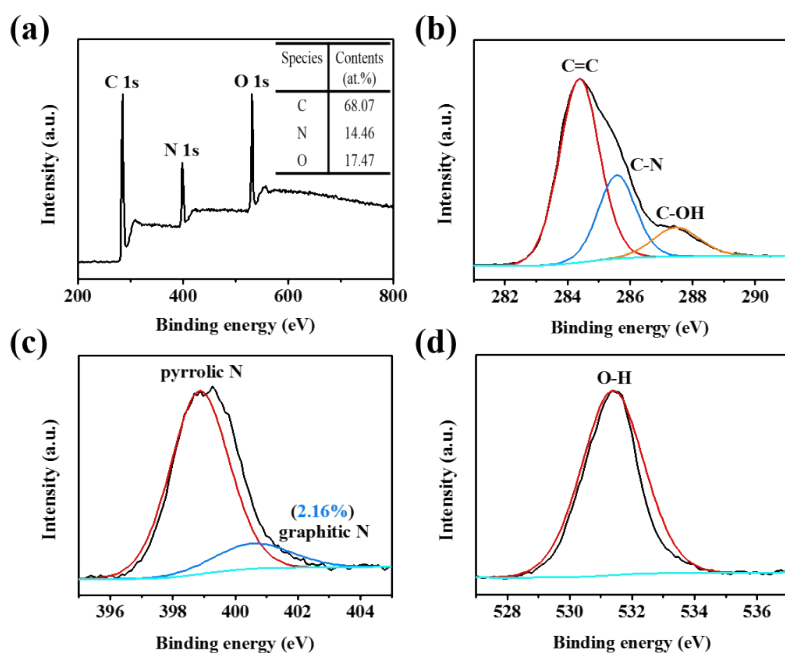


Fig. S1 (a) Survey XPS spectrum of the NIR-CD₁₈₀₀. (b) XPS C 1s spectrum of the NIR-CD₁₈₀₀. (c) XPS N 1s spectrum of the NIR-CD₁₈₀₀. (d) XPS O 1s spectrum of the NIR-CD₁₈₀₀.

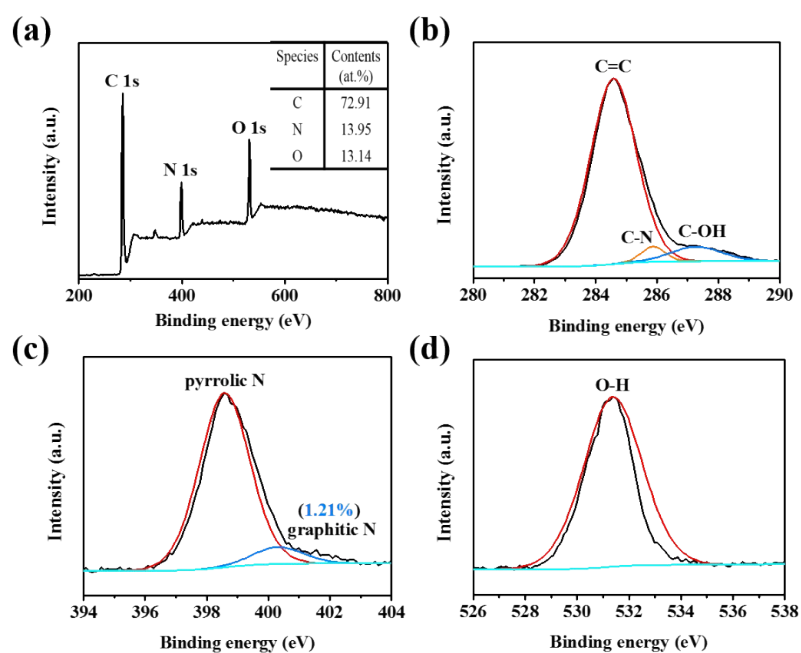


Fig. S2 (a) Survey XPS spectrum of the NIR-CD₆₀₀. (b) XPS C 1s spectrum of the NIR-CD₆₀₀. (c) XPS N 1s spectrum of the NIR-CD₆₀₀. (d) XPS O 1s spectrum of the NIR-CD₆₀₀.

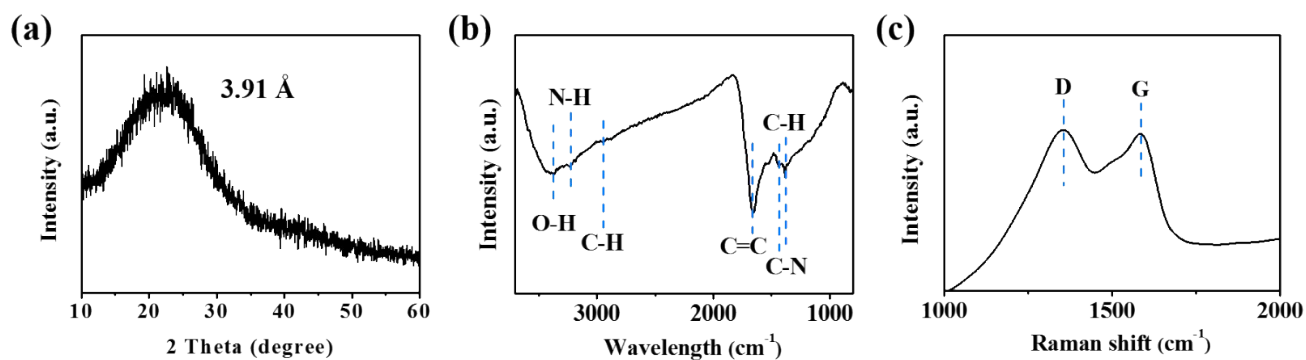


Fig. S3 XRD (a), FT-IR (b), and Raman spectrum (c) of the NIR-CDs.

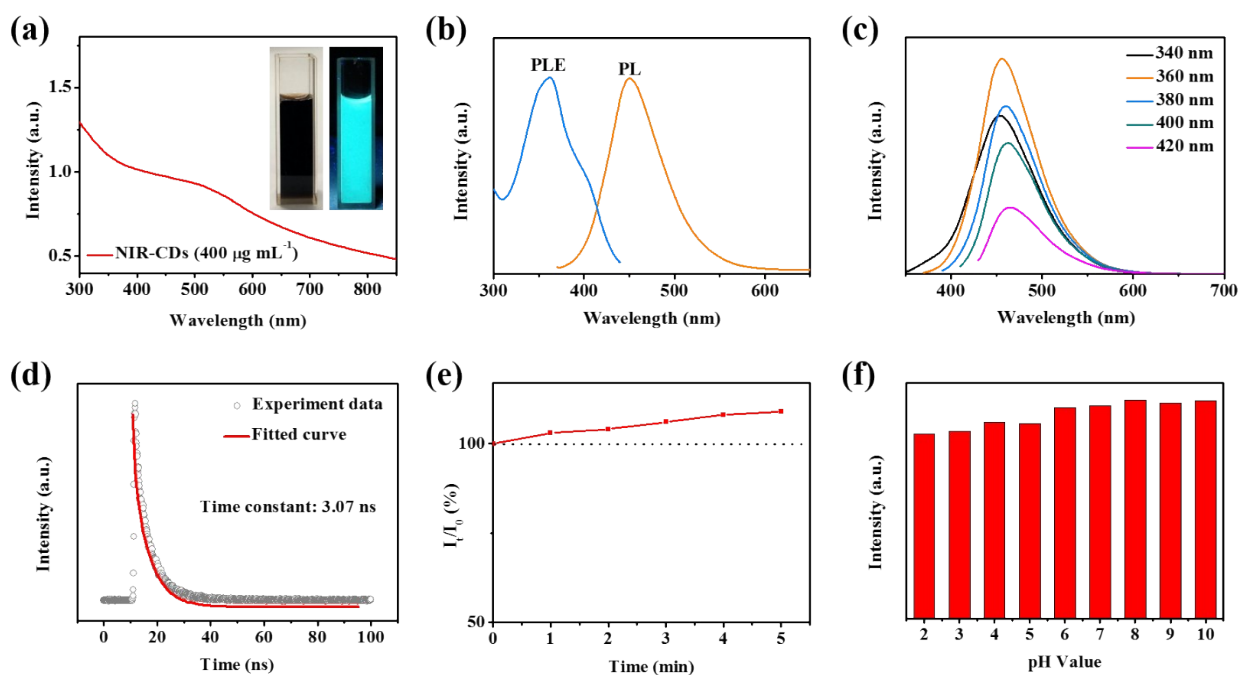


Fig. S4 (a) UV-vis-NIR absorption spectrum of NIR-CD solution (inset: Photographs of NIR-CD solution taken under visible (left) and UV (right) lights). (b) PL and excitation (PLE) spectra of NIR-CDs. (c) PL spectra of NIR-CDs excited at different wavelengths varied from 340 nm to 420 nm. (d) Time-resolved PL spectrum of NIR-CDs. (e) Photostability test under 5-h continuous radiation using a 100 W xenon lamp. (f) Dependence of PL intensity on pH values.

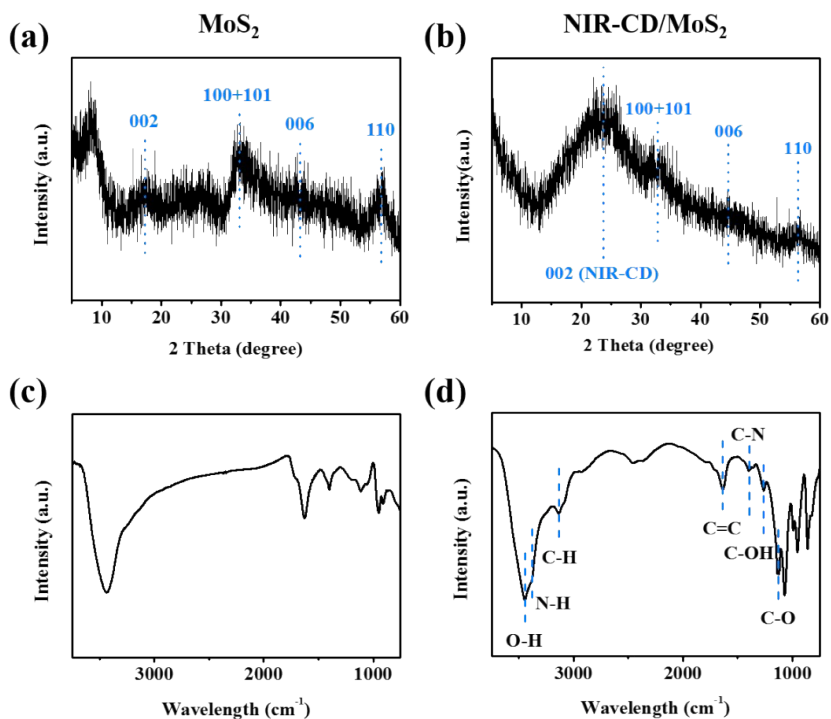


Fig. S5 XRD spectrum and FT-IR spectrum of MoS₂ (a,c) and NIR-CD/MoS₂ heterojunctions (b,d).

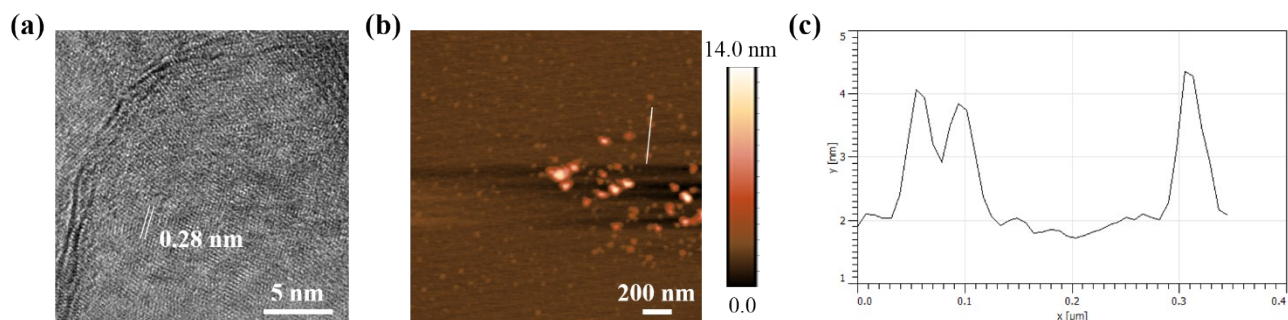


Fig. S6 (a) HRTEM image of MoS₂ nanosheets. (b-c) AFM image and height profile of NIR-CD/MoS₂ heterojunctions.

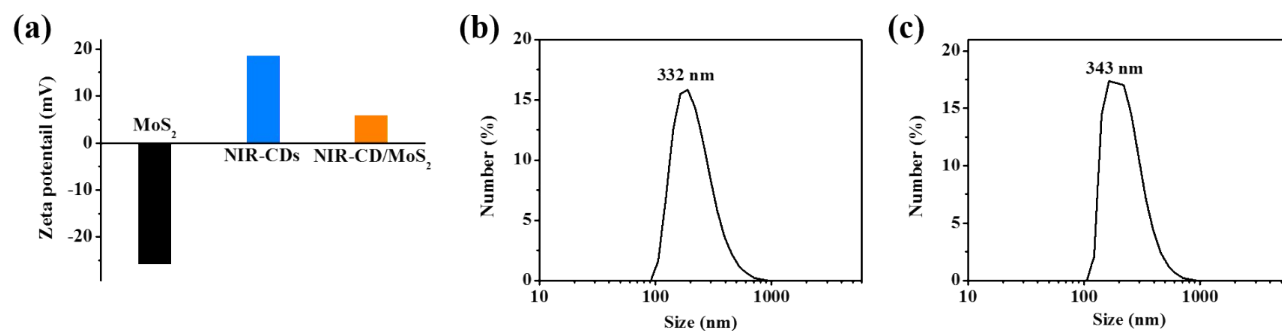


Fig. S7 (a) Zeta potential of MoS₂, NIR-CDs, and NIR-CD/MoS₂ heterojunctions. Dynamic light scattering (DLS) spectrum of MoS₂ (b) and NIR-CD/MoS₂ (c).

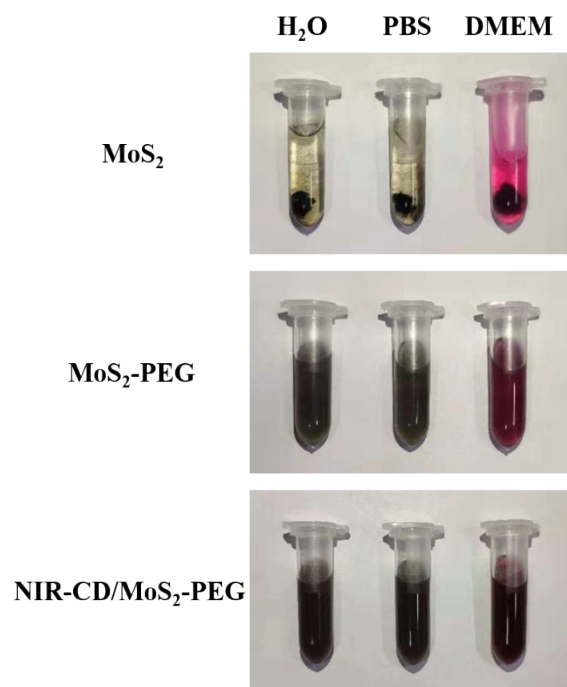


Fig. S8 Photos of MoS₂, MoS₂-PEG, and NIR-CD/MoS₂-PEG in water, PBS and cell medium (DMEM) after 3,000 rpm centrifugation.

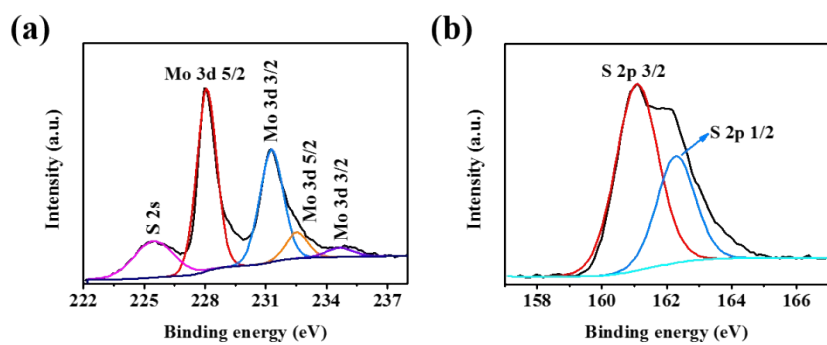


Fig. S9 High-resolution Mo 3d (a) and S 2p (b) spectra of the NIR-CD/MoS₂ heterojunctions.

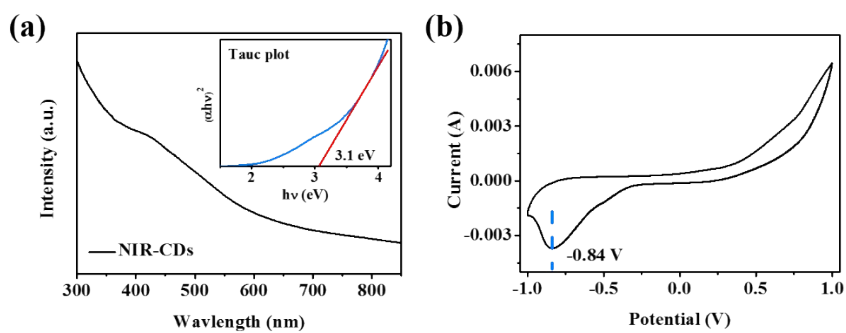


Fig. S10 (a) UV-vis-NIR absorption spectrum and Tauc plot of the NIR-CDs. (b) CV curve of NIR-CDs.

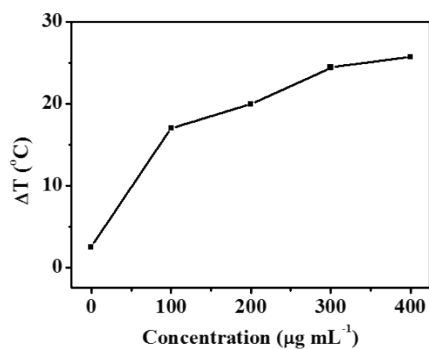


Fig. S11 Plot of temperature change (ΔT) over a period of 300 s versus different concentrations of NIR-CD/MoS₂.

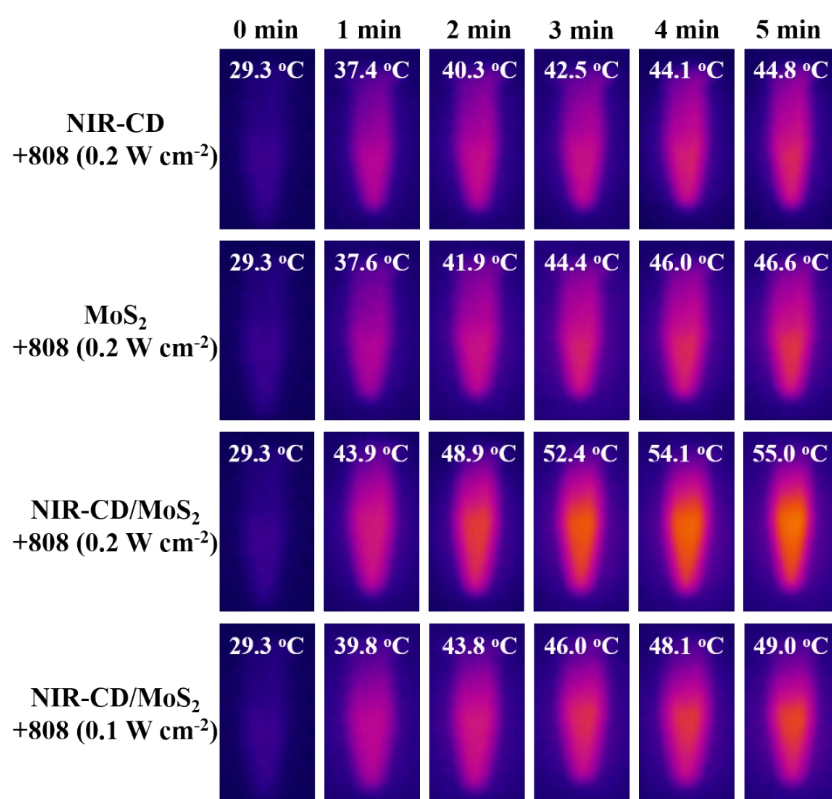


Fig. S12 Infrared thermographic images of centrifuge tubes filled with NIR-CDs (600 $\mu\text{g mL}^{-1}$), MoS₂ (600 $\mu\text{g mL}^{-1}$), and NIR-CD/MoS₂ (600 $\mu\text{g mL}^{-1}$) were measured at 0-5 min with an IR camera after continuous laser irradiation at a power density of 0.2 W cm⁻².

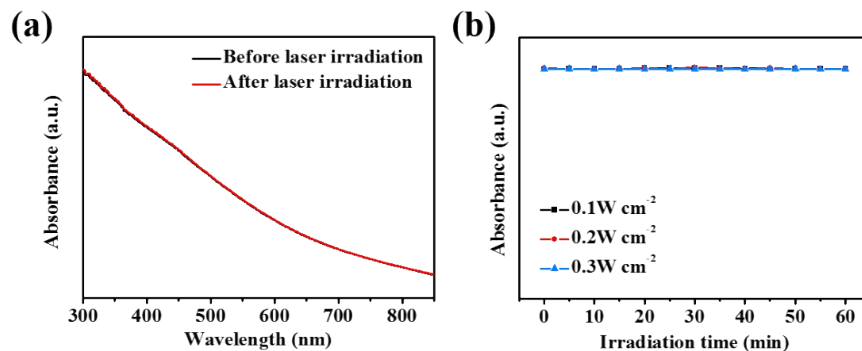


Fig. S13 (a) UV-vis-NIR absorption spectra of NIR-CD/MoS₂ before and after laser irradiation (0.2 W cm⁻² for 60 min). (b) Change of absorbance at 808 nm for NIR-CD/MoS₂ solutions under laser exposure at different power densities (0.1, 0.2, 0.3 W cm⁻²) for 60 min.

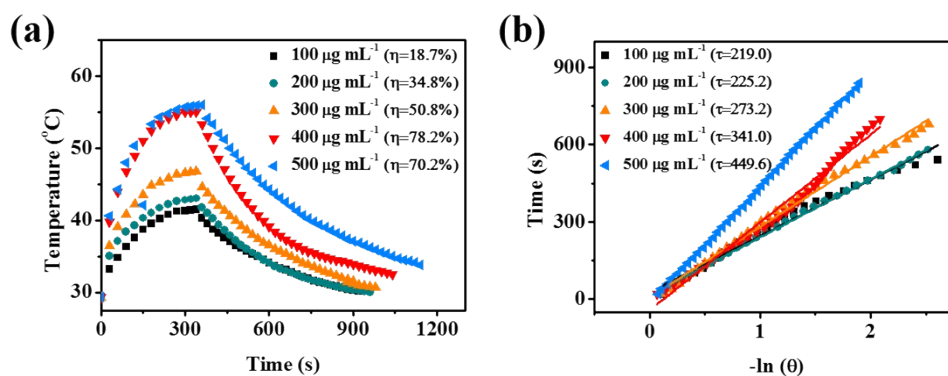


Fig. S14 The photothermal effect of NIR-CD/MoS₂ with varied NIR-CD loading level under illumination with an 808 nm laser (0.2 W cm⁻²), the concentration of NIR-CDs varied from 100 to 500 μg mL⁻¹. (e) Plot of cooling time versus negative natural logarithm of the temperature driving force obtained from the cooling period.

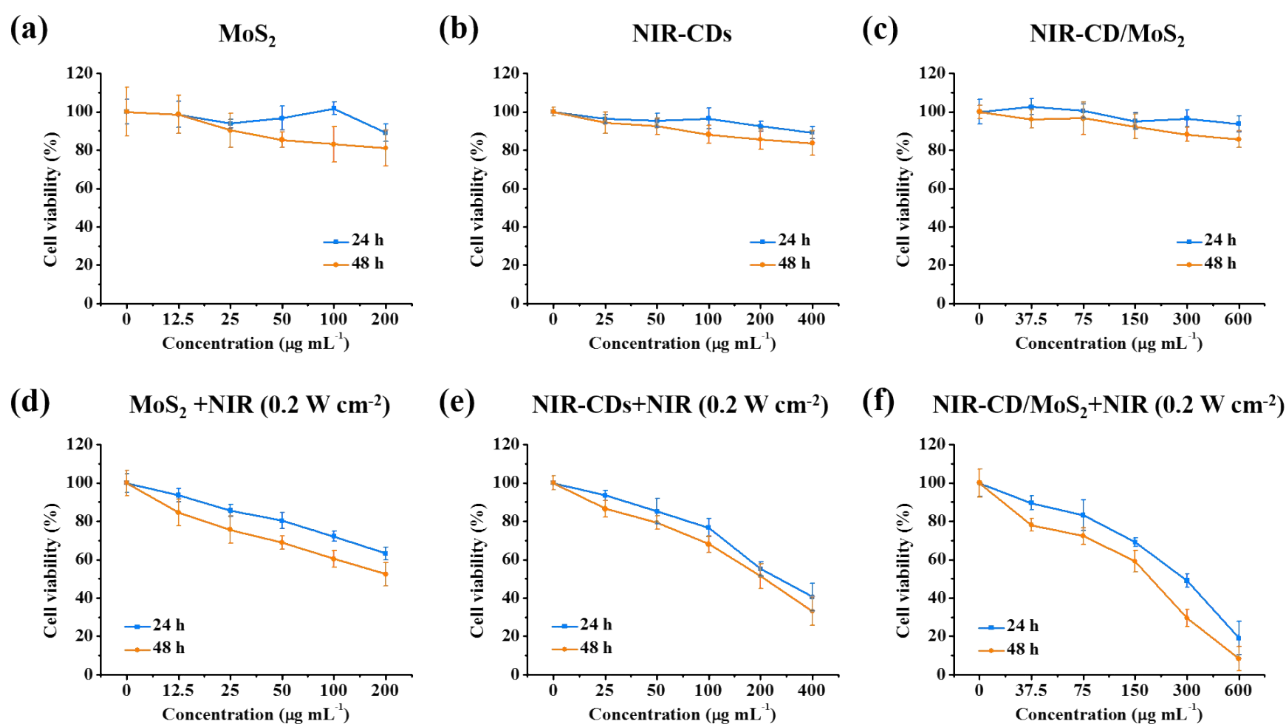


Fig. S15 In vitro cytotoxicity of MoS₂ (a and d), NIR-CDs (b and e), and NIR-CD/MoS₂ (c and f) against HeLa cells after incubation for 24 h and 48 h with and without NIR laser irradiation (808 nm, 0.2 W cm⁻²), respectively. The concentration of MoS₂ was 0, 0.0125, 0.025, 0.05, 0.1, and 0.2 mg mL⁻¹. The concentration of NIR-CDs was 0, 0.025, 0.05, 0.1, 0.2, and 0.4 mg mL⁻¹. The concentration of NIR-CD/MoS₂ was 0, 0.0375, 0.075, 0.15, 0.3, and 0.6 mg mL⁻¹.

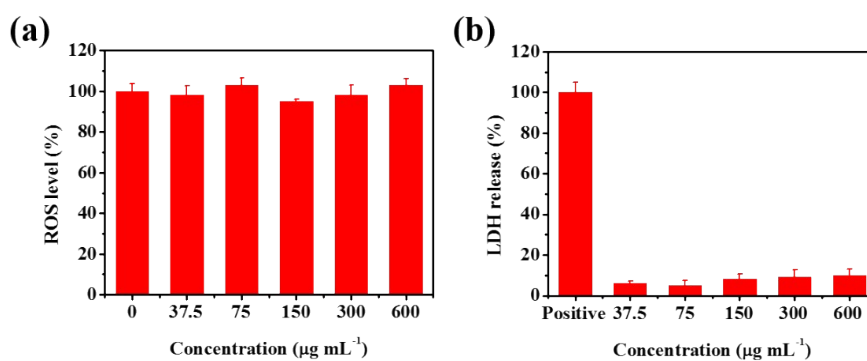


Fig. S16 (a) ROS level of HeLa cells after incubation with NIR-CD/MoS₂ at various concentrations. (b) Released LDH in cell culture supernatants after incubation of HeLa cells with NIR-CD/MoS₂. Error bars are based on six parallel samples.

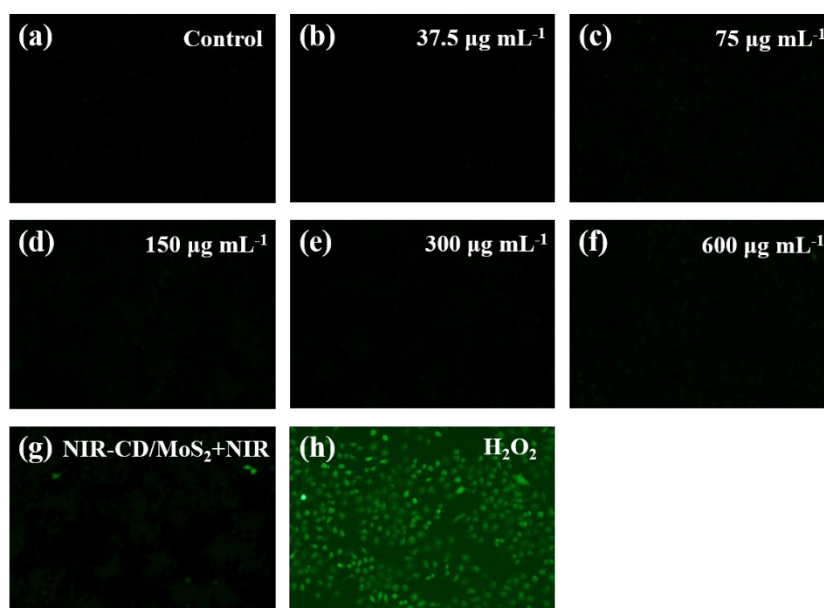


Fig. S17 Observation by fluorescence microscope images of ROS in cancer cells that received different treatments. (a) Untreated cells, (b-f) cells treated with NIR-CD/MoS₂ at different concentration (37.5-600 μg mL⁻¹), (g) cells treated with NIR-CD/MoS₂ plus NIR irradiation (0.2 W cm⁻², 5 min), (h) cells treated with H₂O₂ as a positive control.

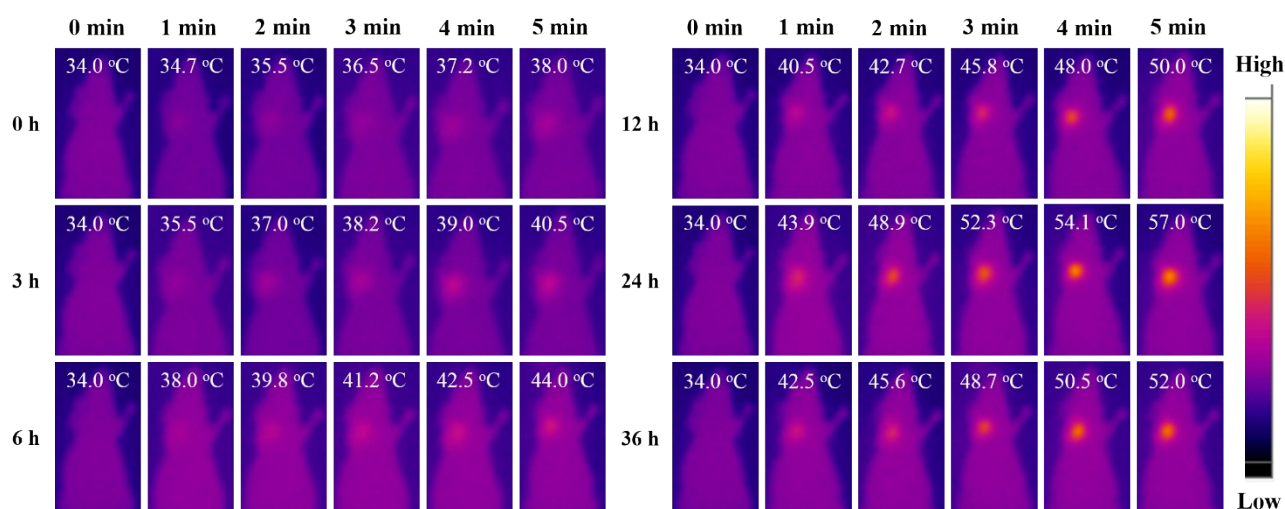


Fig. S18 Maximum temperature within the tumor region recorded by an IR camera after intravenous injection of NIR-CD/MoS₂ and 808 nm laser irradiation at different time points (0, 3, 6, 12, 24, and 36 h).

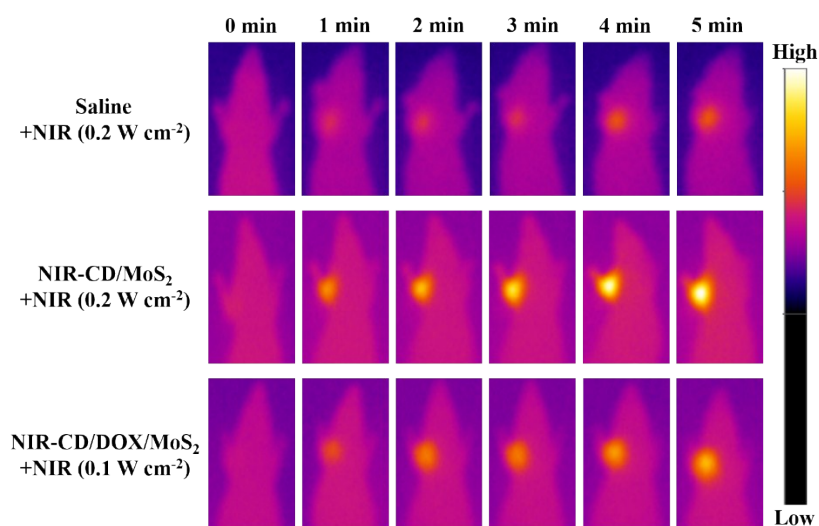


Fig. S19 Maximum temperature within the tumor region recorded by an IR camera after systematic administration and 808 nm laser irradiation.

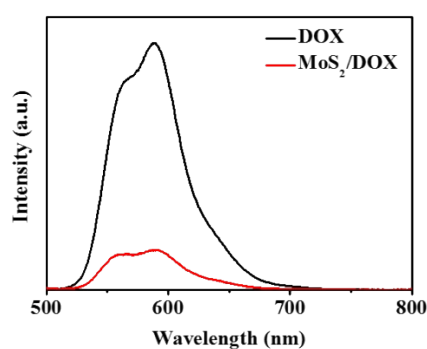


Fig. S20 Fluorescent spectra of free DOX and MoS₂/DOX aqueous solutions at the same DOX concentration (λ_{ex} =480 nm).

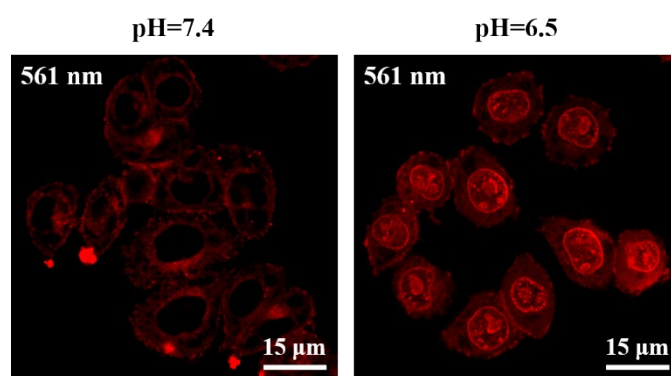


Fig. S21 Confocal fluorescence images of HeLa cells incubated with NIR-CD/DOX/MoS₂ at pH=7.4 and 6.5.

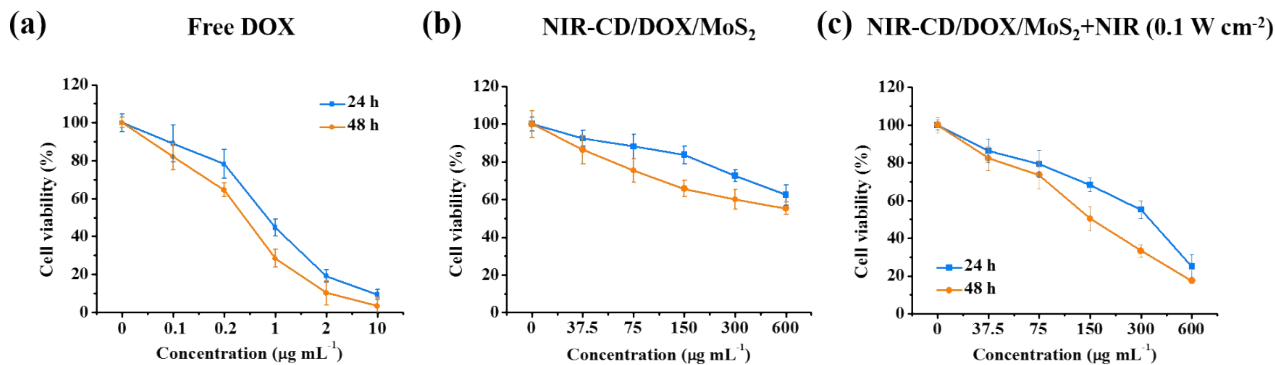


Fig. S22 (a) In vitro cytotoxicity of free DOX against Hela cells after incubation for 24 h and 48 h without NIR laser irradiation. The concentration of DOX was 0, 0.1, 0.2, 1, 2, and 10 µg mL⁻¹. (b, c) In vitro cytotoxicity of NIR-CD/DOX/MoS₂ against Hela cells after incubation for 24 h and 48 h with and without NIR laser irradiation (808 nm, 0.1 W cm⁻²), respectively. The concentration of NIR-CD/DOX/MoS₂ was 0, 0.0375, 0.075, 0.15, 0.3, and 0.6 mg mL⁻¹.

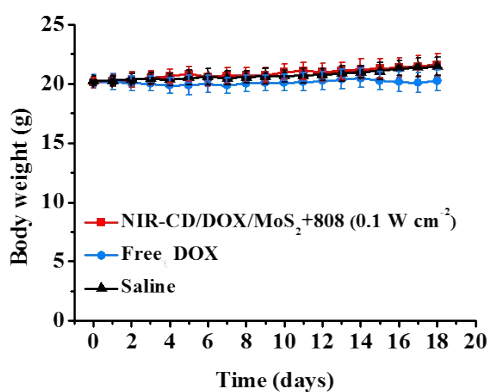


Fig. S23 Monitoring curves of the body weight of mice over the whole treatment period.

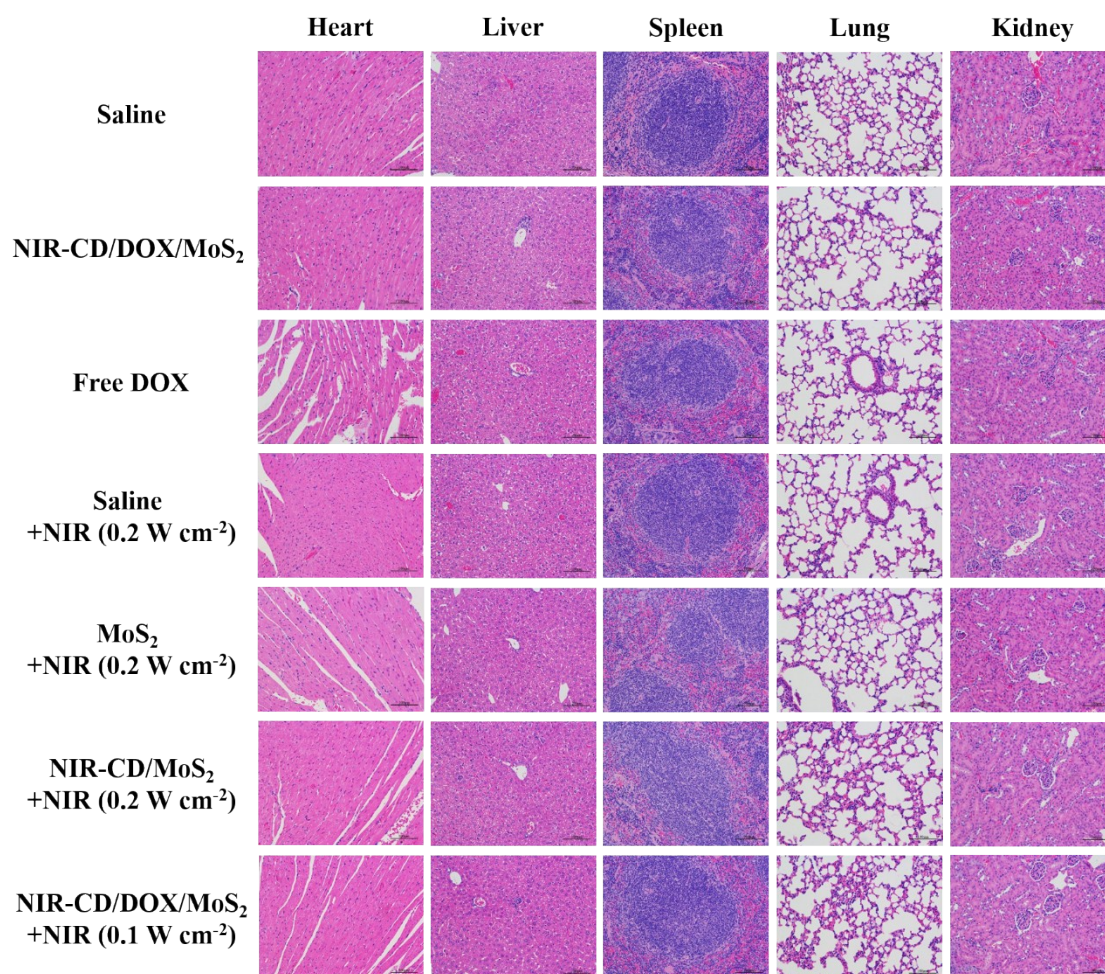


Fig. S24 H&E staining images of major organs including heart, liver, spleen, lung, kidney. The organs were collected from the Balb/c mice that were sacrificed at 18 days after intravenously injected of saline, NIR-CD/MoS₂, free DOX, saline+NIR (0.2 W cm⁻²), MoS₂+NIR (0.2 W cm⁻²), NIR-CD/MoS₂+NIR (0.2 W cm⁻²), and NIR-CD/DOX/MoS₂ +NIR (0.1 W cm⁻²), respectively.

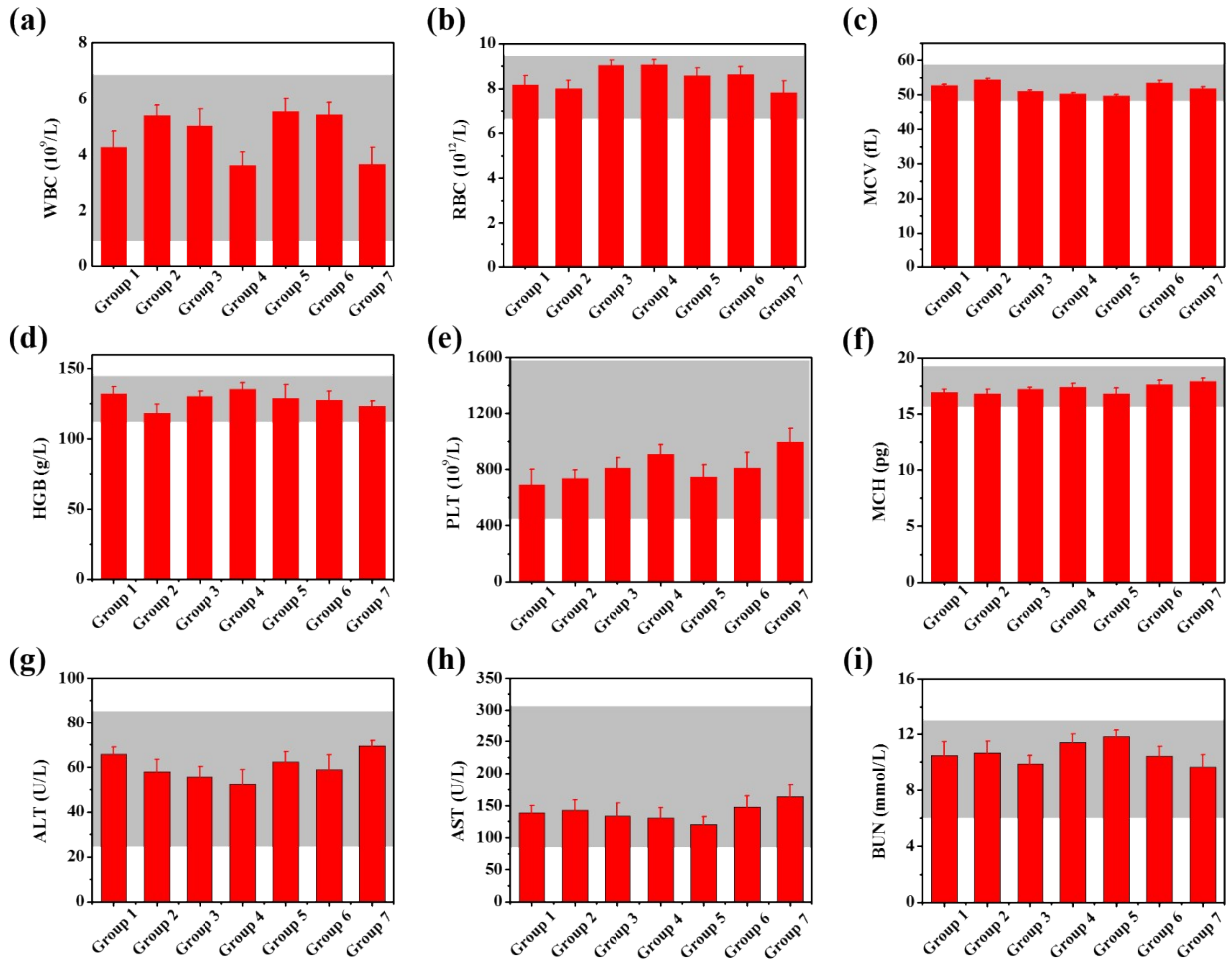


Fig. S25 The whole blood was collected from the Balb/c mice that were sacrificed at 18 days after intravenously injected of saline (group 1), NIR-CD/MoS₂ (group 2), free DOX (group 3), saline+NIR (0.2 W cm⁻²) (group 4), MoS₂+NIR (0.2 W cm⁻²) (group 5), NIR-CD/MoS₂+NIR (0.2 W cm⁻²) (group 6), and NIR-CD/DOX/MoS₂+NIR (0.1 W cm⁻²) (group 7), respectively. Hematology data: (a) white blood cells (WBC), (b) red blood cells (RBC), (c) mean corpuscular volume (MCV), (d) hemoglobin (HGB), (e) platelet (PLT), and (f) Mean corpuscular hemoglobin (MCH). Serum biochemistry data: (g) alanine aminotransferase (ALT), (h) aspartate aminotransferase (AST), and (i) Urea nitrogen (BUN).

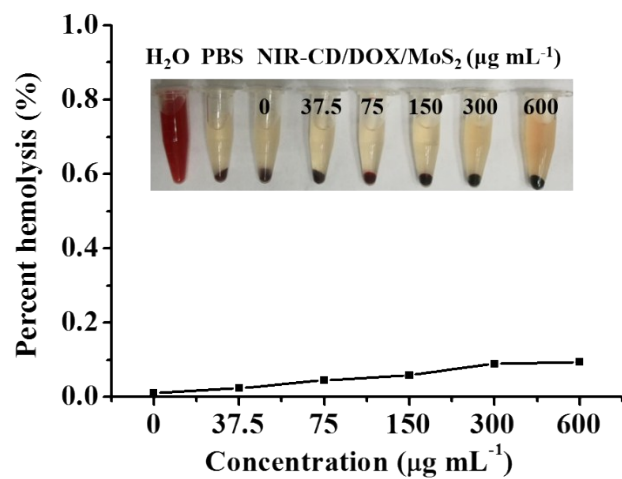


Fig. S26 Hemolytic percentages of RBCs treated with different concentrations of NIR-CD/DOX/MoS₂ solution for 3 h. The inset images are for direct observation of the results, suggesting the good biocompatibility of NIR-CD/DOX/MoS₂ heterojunctions.